J Bioenerg Biomembr (2008) 40:359–369
DOI 10.1007/s10863-008-9162-x

# Nuclear and mitochondrial subunits from the white shrimp *Litopenaeus vannamei* $F_0F_1$ ATP-synthase complex: cDNA sequence, molecular modeling, and mRNA quantification of *atp9* and *atp6*

**Adriana Muhlia-Almazan · Oliviert Martinez-Cruz · Ma. de los Angeles Navarrete del Toro · Fernando Garcia-Carreño · Rodrigo Arreola · Rogerio Sotelo-Mundo · Gloria Yepiz-Plascencia**

Received: 11 March 2008 / Accepted: 16 May 2008 / Published online: 4 September 2008


**Abstract** We studied for the first time the ATP-synthase complex from shrimp as a model to understand the basis of crustacean bioenergetics since they are exposed to endogenous processes as molting that demand high amount of energy. We analyzed the cDNA sequence of two subunits of the Fo sector from mitochondrial ATP-synthase in the white shrimp *Litopenaeus vannamei*. The nucleus encoded *atp9* subunit presents a 773 bp sequence, containing a signal peptide sequence only observed in crustaceans, and the mitochondrial encoded *atp6* subunit presents a sequence of 675 bp, and exhibits high identity with homologous sequences from invertebrate species. *ATP9* and *ATP6* protein structural models interaction suggest specific functional characteristics from both proteins in the mitochondrial enzyme. Differences in the steady-state mRNA levels of *atp9* and *atp6* from five different tissues correlate with tissue function. Moreover, significant changes in the mRNA levels of both subunits at different molt stages were detected. We discussed some insights about the enzyme structure and the regulation mechanisms from both ATP-synthase subunits related to the energy requirements of shrimp.

**Keywords** ATP-synthase · Mitochondrial genes · Nuclear genes · Shrimp · Subunit *atp6* · Subunit *atp9*

A. Muhlia-Almazan (✉) · O. Martinez-Cruz · R. Sotelo-Mundo · G. Yepiz-Plascencia
Molecular Biology Lab. Centro de Investigación en Alimentación y Desarrollo (CIAD), A. C.,
Carretera a La Victoria Km 0.6, P.O. Box. 1735, Hermosillo, Sonora 83000, Mexico
e-mail: amuhlia@ciad.mx

M. d. l. A. Navarrete del Toro · F. Garcia-Carreño
Biochemistry Lab. Centro de Investigaciones Biologicas del Noroeste (CIBNOR), S.C.,
Mar Bermejo 195. Col. Playa Palo de Santa Rita,
P.O. Box 128, La Paz, Baja California Sur 23090, Mexico

R. Arreola
Department of Biotechnology and Bioengineering,
Centro de Investigación y de Estudios Avanzados del IPN (CINVESTAV-IPN),
Mexico City 07360, Mexico

## Introduction

The mitochondrial $F_0F_1$-ATP synthase (EC 3.6.1.34) is the last enzymatic complex of the electron transport chain and is responsible for ATP synthesis and hydrolysis. The enzyme is comprised by two major sectors, the Fo, the hydrophobic transmembrane portion, and the F1, the hydrophilic segment exposed to the mitochondrial inner matrix (Boyer 1997). The complex is driven by a proton gradient, where two sectors functionally interact as "motors" in such a way that catalysis is dependent on the cooperation of both sectors (Boyer 1997; Wang and Oster 1998; Vick and Ishmukhametov 2005). This multimeric complex of the oxidative phosphorylation pathway is formed by several subunits encoded in two physically separated genomes, the mitochondrial and the nuclear (Godbout et al. 1993; Itoi et al. 2003). The Fo sector includes a core unit that is composed of $ac_{10-14}$ molecules (Hong and Pedersen 2003), including 10–13 molecules of subunit *c* in bacteria (also called subunit 9 in eukaryotes) encoded in the nucleus, and a single copy of subunit *a* in bacteria (named subunit 6 in

eukaryotes) encoded in the mitochondria. All the subunits encoded in the nucleus are translated on cytoplasmic ribosomes, often as large precursors carrying N-terminal targeting pre-sequences, that are imported into the mitochondria and then assembled to form the multimeric complex (Andersson et al. 1997; Itoi et al. 2003; Sangawa et al. 1997).

Genes from nuclear subunits of the Fo domain in the ATP-synthase have been deeply studied from vertebrate species such as rat (DeWoody et al. 1999; Yotov and St-Arnaud 1993), cow (Gay and Walker 1985), and human (Dyer and Walker 1993), and scarce information has been reported for invertebrates (Caggese et al. 1999; Sardiello et al. 2005). In marine shrimp species, only three genes from nuclear subunits of the ATP-synthase complex have been recently identified when evaluating gene expression profiles using cDNA microarrays or libraries from shrimp tissues at different physiological conditions (Wang et al. 2006; Brown-Peterson et al. 2008), however, no exclusive efforts have been done to study crustacean species ATP-synthase subunits, specially *ATP9*.

The *atp6* subunit is one of the two subunits encoded in the mitochondrial genome as reported in several crustacean species including shrimp *Penaeus notialis* (GenBank X84350; Garcia-Machado et al. 1996), *P. monodon* (GenBank AF217843; Wilson et al. 2000), and *Litopenaeus vannamei* (GenBank NC_009626; DQ534543; Shen et al. 2007). The complete cDNA sequence of *atp6* has not been reported for shrimp species, although there are several reports of crustacean complete mitogenomes.

In crustaceans, physiological processes such as molting require high amounts of energy. It is well documented that during molting, energy reserves in the midgut gland are depleted since it implies obligated starvation (Dall et al. 1990; Muhlia-Almazan and Garcia-Carreño 2002). Starvation produces changes in the midgut gland of shrimp, especially in the mRNA levels of nuclear genes such as trypsin, and mitochondria-encoded genes like *16SrRNA* at different molt stages (Sanchez-Paz et al. 2003).

In the present work we studied and refer to *atp6* as the mitochondria-encoded subunit, and to *atp9* as the nuclear-encoded subunit. We closely analyzed, for the first time, these specific subunits of the mitochondrial $F_0F_1$ ATP-synthase complex from the Pacific white shrimp *L. vannamei*, to obtain basic information as their complete cDNA sequences and their predicted molecular protein models. We also evaluated the steady state mRNA levels of both subunits in different shrimp tissues, and in shrimp at different molting stages to obtain insights about energy production proteins related to tissues function and molting. We also compared the expression of the nucleus and mitochondria-encoded ATP-synthase subunits and discuss the existence of mechanisms coordinating these genes expression in shrimp.

## Materials and methods

### Animals

Twenty eight adult male *L. vannamei* shrimp were obtained from intertidal ponds at CIBNOR, La Paz, BCS, México. They were selected by size and molt stage, individually dissected and tissues were used as explained below.

### *Atp9* and *atp6* cDNA sequencing

Five μg of total RNA from midgut gland of five individual shrimp were used to synthesize cDNA to sequence the complete transcripts of *atp9* and *atp6* subunits. cDNA was synthesized using 1 μL (10 mM) dNTP mix, 1 μL (0.50 μg/μL) oligo dT and DEPC-treated water to adjust to a 10 μL reaction mixture. The reaction mixture was incubated for 5 min at 65 °C and then placed on ice for 2 min. Then, 2 μL (10×) RT buffer, 4 μL (25 mM) $MgCl_2$, 2 μL (0.1 M) dithiotreitol (DTT), 1 μL RNase inhibitor, and 1 μL (50 units) Superscript II™ reverse transcriptase were added to a final reaction volume of 20 μL and incubated for 50 min at 42 °C.

Specific oligonucleotides were designed for each ATP-synthase subunit (Table 1), based on ESTs sequences available at the GenBank (*atp9*, BE188603; *atp6*, AF217843). PCR amplifications of cDNA fragments encoding *atp9*, and *atp6* subunits were carried out in 50 μl reactions containing: 5 μL (10×) PCR buffer, 6 μL (25 mM) $MgCl_2$, 2 μL (10 mM) dNTP mix, 0.8 μM of each oligonucleotide, 2 μL of cDNA and 2 U of *Taq* DNA polymerase. A thermocycler (PTC 200 DNA Engine, MJ

**Table 1** Specific oligonucleotides used to amplify shrimp Fo ATP-synthase subunits *atp9*, *atp6,* and *L8* genes

| Gene | Label | Sequence |
|---|---|---|
| Nuclear genes | | |
| *atp9* | ATP9FwCAM | 5′-tcgatcatcagatcaacacaca-3′ |
| *atp9* | ATP9Fw2CAM | 5′-cgagtaggcaatgtcaaac-3′ |
| *atp9* | ATP9Fw3CBRT | 5′-aattggatccgtctttggttcc-3′ |
| *atp9* | ATP9RvCAM | 5′-ttagaaagcgaaaagcaacagg-3′ |
| *L8* | L8Fw3 | 5′-taggcaatgtcatccccatt-3′ |
| *L8* | L8Rv3 | 5′-tcctgaaggaagctttacacg-3′ |
| Mitochondrial genes | | |
| *atp6* | ATP6FwCAM | 5′-cagtttttgatcctacktcaa g-3′ |
| *atp6* | ATP6Fw2CBRT | 5′-gctcatcttgttccgcaagg-3′ |
| *atp6* | ATP6Rv1CAM | 5′-cggcaaaaacatatgattgaa-3′ |
| *atp6* | ATP6Rv2CAM | 5′-tccctggtcggataacattt-3′ |
| *atp6* | ATP6Rv3CBRT | 5′-ctgctaatcgcactgctaagg-3′ |
| *cox3*[a] | CO3RvCAM | 5′-tatcaygcggcagcttcaaat-3′ |
| *cox2*[a] | CO2Fw2CAM | 5′-aggkcttaatggwatacctcgacg-3′ |

[a] Oligonucleotides designed to amplify the flanking genes (CO2 and CO3) of the mitochondrial ATP6 gene.

Research) was used with the following conditions: 1 min at 95 °C (one cycle); 30 s at 95 °C, 1 min at 60 °C and 1 min at 72 °C (29 cycles); and an over-extension step for 10 min at 72 °C. The resulting PCR products were analyzed in 1.2% agarose gels and stained with ethidium bromide (Sambrook and Russell 2001). PCR products were purified and sequenced. The complete cDNA sequence of subunit *atp9* was obtained using a primer walking strategy (Table 1).

To obtain the full length cDNA sequence of the mitochondrial *atp6* subunit, specific oligos were designed based on the reported sequences from the flanking genes of *atp6* gene, *cox2* and *cox3* in the mitogenome of *Penaeus monodon* (GenBank, AF217843; Table 1). Larger PCR products including the complete sequence of *atp6* were obtained using cDNA as template under the above mentioned conditions and were purified and sequenced.

Additional information was obtained from clones isolated from a hemocytes cDNA unidirectional library constructed in our lab in the SMART system (Clontech, Palo Alto, CA, USA). The full length cDNA sequences of *atp9* and *atp6* were confirmed by repeatedly sequencing both strands from different individual shrimp by the dideoxy chain-termination method at the Laboratory of Molecular and Systematic Evolution at The University of Arizona. Completed sequences were compared to nucleotide and protein data bases using the BLAST algorithm (N and P; Altschull et al. 1990).

## Molecular modeling of the *ATP9* and *ATP6* deduced amino acid sequence

Shrimp *ATP9* and *ATP6* protein models were built based on the 1C17 PDB file coordinates. This file contains the structural coordinates of an $a_1c_{12}$ subcomplex of F1Fo ATP-synthase from *E. coli*. The *c* subunits formed a dodecameric ring and one *a* subunit was bound to two *c* subunits. In the structure obtained from NMR data, the conformational changes linked to proton translocation by subunits *a*–*c* were deduced (Rastogi and Girvin 1999). Based on that model, a theoretical shrimp *ATP9-ATP6* model was built comprising three *ATP9* and one *ATP6* subunits.

The *ATP6* model was built using homology modeling as implemented in SwissModel using chain M of 1C17. The sequence alignment of the *ATP6* sequences was straightforward, but for *ATP9* it was complicated since the modeling involved two different conformations related to proton translocation, using chain A, and K of 1C17. Therefore the models contain the same amino acid sequence but different conformation, and were manually corrected using the "O" structural software (Jones et al. 1991). The structural model was not structurally minimized to improve geometry parameters due to the low similarity with the target sequence.

## *Atp9* and *atp6* mRNA determination by qRT-PCR

To evaluate mRNA levels from different shrimp tissues, three adult male (*L. vannamei*) weighting 37–38 g were selected at intermolt stage, killed and the midgut gland (MG), muscle (M), pleopods (PL), and gills (G) individually dissected and stored in RNA-later reagent (Ambion, Austin, TX) at −20 °C until use. Haemolymph samples were obtained from the ventral side of the pleopod, by puncture at the first abdominal segment using a 1 mL insulin syringe containing one volume of anticoagulant solution (450 mM NaCl, 10 mM KCl, 20 mM EDTA $Na_2$, 10 mM HEPES, pH 7.3; Vargas-Albores et al. 1993). Hemocytes from each sample were separated by centrifugation for 5 min at 600 × *g*, at room temperature, and cell pellets were suspended in 50 μL of RNA-later reagent.

To evaluate mRNA levels of *atp9* and *atp6*, 20 adult male (18–22 g) were selected by setogenesis (Chan et al. 1988) in the following molt stages: A/B (postmolt); C (intermolt); EP (early premolt including stages $D_0$–$D_1$), and LP (late premolt including stages $D_2$–$D_3$). Five organisms from each stage were individually decapitated and the midgut gland, which is the main fuel storage organ from shrimp, were dissected and frozen in liquid nitrogen, then stored at −20 °C until use.

## Total RNA extraction and cDNA synthesis

All tissues dissected for mRNA evaluation were homogenized in TRIzol (Invitrogen, Carlsbad, CA), to isolate total RNA according to manufacturer instructions. Total RNA concentration was determined and analyzed in a 1.2% formaldehyde-agarose gel electrophoresis (Sambrook and Russell 2001). Contaminating DNA was removed using DNAse I (Sigma; 1 U/ μg RNA) according to manufacturer instructions. Complementary DNA (cDNA) was synthesized from 7 μg of total RNA using the Superscript first-strand synthesis system for RT-PCR and random hexamers (Invitrogen, Carlsbad, CA). cDNA samples were used to evaluate mRNA levels.

## qRT-PCR by real time

The mRNA steady state levels from *atp6* and *atp9* were determined using an iQ5 multicolor real-time PCR detection system (BioRad, CA, USA). Specific gene oligonucleotides were designed to amplify *atp9* (ATP9Fw3CBRT and ATP9RvCAM), and *atp6* fragments (ATP6Fw2CBRT and ATP6Rv3CBRT). The ribosomal protein *L8* was used as an internal control gene (GenBank DQ316258), to normalize *atp9* and *atp6* expression (Table 1). Real time PCR amplifications were done in triplicates. Total volume reactions of 25 μL were prepared including 12.5 μL of 2× iQ SYBR Green supermix (BioRad, CA, USA), 0.8 μM each of forward

and reverse oligonucleotides, and cDNA synthesized from 700 ng of total RNA from each individual sample. PCR conditions were: 95 °C for 5 min followed by 40 cycles at 95 °C for 30 s, 60 °C *atp6*/63 °C *atp9* and *L8* for 35 s, 68 °C for 55 s with a final melting curve program from 60 °C to 95 °C increasing 0.3 °C each 20 s. Fluorescence readings were taken at 68 °C after each amplification cycle.

Standard curves were constructed for each gene using purified PCR products as template. Ten-fold serial dilutions were done from 0.25 ng to $2.5\times10^{-9}$ ng for *atp9*, *atp6*, and *L8* standard curves. PCR efficiency (%) was calculated for each fragment and compared between them to be equal, and used to calculate the relative expression ratio (ER) method reported by Bacca et al. (2005), to evaluate mRNA levels. The calculation is based on the threshold value (CT) of each sample and the formula $ER=2^{-(CTatp\ \ gene\text{-}CTL8)}$. Results are expressed as the copy number of each *atp* transcript relative to the reference ribosomal protein *L8*. Data obtained from different tissues or molt stages were analyzed by median comparisons using the Kruskal–Wallis ANOVA by ranks, and the Mann–Whitney *U* tests performed with Statistica 6.0 software.

## Results

### *Atp9* cDNA sequence

The full length cDNA sequence of *atp9* from shrimp *L. vannamei* (GenBank EU194608) was determined. The complete sequence is 773 bp long, and it includes a 67 bp 5′-untranslated region (UTR) sequence, a coding region of 351 bp with the start (ATG) and (TAA) stop codons, a 123 bp sequence coding for the signal peptide sequence, the region coding the mature protein of 228 bp, and finally a 355 bp long -3′ UTR sequence that commonly characterizes shrimp transcripts (Clavero-Salas et al. 2007). Three putative ATTTA-rich regions regulating mRNA stability were found in the -3′ UTR end, the first of them is suggested to be a polyadenylation signal since *atpc* or *atp9* transcripts commonly do not have a clear polyadenylation signal in some other species (Viebrock et al. 1982; Dyer and Walker 1993; Malter and Hong 1991; Fig. 1A). The *atp9* cDNA sequence of *L. vannamei* has high identity to invertebrate homologs as the tobacco hornworm *Manduca sexta* mRNA (88%, AF117583), other arthropod species *as Dermacentor variabilis* mRNA (84%, AY241961), and the only one *atp9* partial sequence reported from shrimp species, *Marsupenaeus japonicus* (93%, AB079892). The nucleotide alignment of *atp9* from both shrimp species has high identity in the entire sequence, even in the 5′ and 3′ UTRs, and in the nucleotidic sequence of pre-protein (alignment not shown). The signal peptide sequence is suggested to direct nuclear encoded proteins to the mitochondrial membrane. The deduced amino acid sequence of the pre-protein *ATP9* is 116 residues long, with a predicted molecular weight of 11.9 kDa. This protein, which is also named proteolipid because of its lipid-binding function and its ability to be dissolved in chloroform-methanol solvents (Nagley 1988), has a signal peptide sequence of 41 residues in the *N*-terminal region, which is predicted to be the mitochondrial import sequence. The mature shrimp protein *ATP9* would then be formed by 75 residues with a predicted molecular weight of 7.6 kDa, and an isoelectric point of 6.23. The mature protein size is similar in vertebrates, invertebrates, and some bacteria (Higuti et al. 1993; Andersson et al. 1997; Hong and Pedersen 2003; Fig. 1B).

The alignment of the *ATP9* protein from shrimp and other species showed that the signal peptides are much less conserved than the mature protein. The size of the signal peptide is more variable among bacteria, yeast, insects, and mammals. In crustaceans as *L. vannamei* and *M. japonicus,* the *ATP9* signal peptide is 41 amino acids long, while in vertebrate species varies from 61 to 68 residues (Higuti et al. 1993; Fig. 1B). The signal peptide that precedes the mature protein of the *ATP9* subunit, includes the initial M residue and has a net positive charge of +6 as commonly observed in mitochondrial proteins.

In the shrimp *ATP9* protein, the last amino acid residue of the putative signal peptide, which is immediately before the putative N-terminus of the mature protein is K, while in vertebrate *ATP9* is R, and *ATPc* from *E. coli* is E. Each of these amino acid residues are part of the putative recognition site for proteolytic processing during the synthesis of the protein (Gay and Walker 1985). In addition, predictions about shrimp *ATP9* using the Mito Prot II software (Claros and Vincens 1996), resulted in a probability for this sequence to be imported to mitochondria of 0.9535. Therefore, the putative signal peptide appears to be indeed a bona fide mitochondrial targeting sequence for *ATP9*, containing highly charged residues that can help to stabilize the lipophilic pre-protein *ATP9* in an aqueous environment (Gay and Walker 1985).

Although, alternatively spliced transcript variants for *atp9* (isoforms P1, P2 or P3) have been identified in human, rat, cow and others (Dyer and Walker 1993), there is no evidence of these type of variants in shrimp. The shrimp *ATP9* mature protein has higher identity to transcript form P2, than to the P1 form from bovine and rat (Andersson et al. 1997; Gay and Walker 1985; Fig. 1B). The existence of different transcript forms or tissue-specific expression of the shrimp *ATP9* remains to be investigated.

### *Atp6* cDNA sequence

The full length cDNA sequence from the *atp6* transcript was assembled from the sequences obtained from five individual shrimp and deposited in the GenBank (EU185331).

**a**

```
ACTCCTGGTCCTCCACCACTGACTACTCGGACGATCGATCATCAGATCAACACACACAACCGCCACCATGTACGCTGCCAGGCTTGCCCTCCCCGCTGCA      100
                                                                  M  Y  A  A  R  L  A  L  P  A  A

AGGACTGTTGCTGTCAGGAGCCAGGTTGTGGCCCGCCCCATGGCTGTGGCCCCTCTGACCCGCAGCTTCCAGACCACCACCACCTCCAAGGACATTGACT      200
R  T  V  A  V  R  S  O  V  V  A  R  P  M  A  V  A  P  L  T  R  S  F  O  T  T  T  T  S  K  D  I  D

CTGCTGCCAAGTTCATTGGTGCTGGCGCTGCCACTGTAGGACTAGCAGGATCTGGTGCTGGAATTGGATCCGTCTTTGGTTCCCTTATCATTGGTTATGC      300
S  A  A  K  F  I  G  A  G  A  A  T  V  G  V  A  G  S  Q  A  C  I  Q  S  V  F  G  S  L  I  I  G  Y  A

CCGCAACCCCTCCCTGAAGCAGCAACTCTTCTCATATGCCATTTTGGGTTTTGCCCTGTCTGAGGCTATGGGTCTGTTCTGTCTTATGATGGCCTTCCTG      400
  R  N  P  S  L  K  O  O  L  F  S  Y  A  I  L  G  F  A  L  S  E  A  M  G  L  F  C  L  M  M  A  F  L

TTGCTTTTCGCCTTCTAAGTGCAACACCTTACTGTGTGGACGGACGCCCCTTTACCATCGGGCAGTGGAAAAGCCAGCATGGTGTTTGTGGGCCACTTCC      500
 L  L  F  A  F

AATTGCTTATTGGGCTGACACGAAAATGACCATCACAATTTAATGATAGGCATTGGAGTATCCTTTTGTCCATGTCGACTTTCCCACTAGGAGAACTTCC      600

CCAGTTTCAATGTGTATATAAGGTCTTAAGTTAAGGCTACTCTTGTCTTGTTGGCACACATGTACCCGAGTAGGCAATGTCAAAACTTAATGGTTTAGCC      700

ATTTATTGCCAAGAGTCAGTTACACACAAGGGTTTTCTCATTGTGTACAGATTCCAATGTATAGAAAATTTAC                                  773
```

**b**

```
                                                                                                  * • *•
Gtheta    ------------------------------------------------------------------MNPIVSAASVVASGLSVGLAAIGPGIGQGT 30
Egracilis ------------------------------------------------------------------MNPIICAASVIGAGLAIGLGAIGPGIGQGT 30
Itartaric ----------------------------------------------------------MDMLFAKTVVLAASAVGAGTAMIAGIGPGVGQGY 34
Hsapiens  -MFACSKFVSTPSLVKSTSQLLSRPLSAVVLKRPEILTDESLSSLAVS-CPLT-SLVSSRSFQTSTISRDIDTAAKFIGAGAAT-VGVAGSGAGIGT 93
Rnorvegic -MYACSKFVSTRSLIRSTSQLLSRPLSAVELKRPQMPTDEGLSCLAVR-RPLT-SLIPSRSFQTSAISRDIDTAAKFIGAGAAT-VGVAGSGAGIGT 93
Btaurus   -MYTCAKFVSTPSLIRRTSTVLSRSLSAVVVRRPETLTDESHSSLAVVPRPLTTSLTPSRSFQTSAISRDIDTAAKFIGAGAAT-VGVAGSGAGIGT 95
Lvannamei -MYAARLALPAARTVAVRSQVVARPMAVAP----------------------------LTRSFQTTTTSKDIDSAAKFIGAGAAT-VGVAGSGAGIGS 68
Mjaponic  -MYAARLALPAARTVAVRSQVVARPLAVAP----------------------------LTRSFQTTTTSKDIDSAAKFIGAGAAT-VGVAGSGAGIGS 68
Msexta    MLSAARLIAPAARSAIFSNAAVVRPLAAVSTQTQLVPAAPAQ-------------LSAVRSFQTTSVTKDIDSAAKFIGAGAAT-VGVAGSGAGIG- 82
Klactis   ------------------------------------------------------------MQLVLAAKYIGAGIST-IGLLGAGIGIAI 28
Ecoli1C17 ------------------------------------------------------------MENLNMDLLYMAAAVMMGLAAIGAAIGIGI 30

                  •**■           •  *•      •        ■
Gtheta    AAAQAVEGIARQPEAEGRIRGTLLLSLAFMESLTIYGLVVALALLFANPFTS---      82
Egracilis ASGKAIEGLARQPEAEGKIRGTLLLSLAFMEALTIYGLVVALAIIFANPFV----      81
Itartaric AAGKAVESVARQPEAKGDIISTMVLGQAVAESTGIYSLVIALILLYANPFVGLLG      89
Hsapiens  VFGSLIIGYARNPFLKQQLFSYAILGFALSEAMGLFCLMVAFLILFAM-------     141
Rnorvegic VFGSLIIGYARNPSLKQQLFSYAILGFALSEAMGLFCLMVAFLILFAM-------     141
Btaurus   VFGSLIIGYARNPSLKQQLFSYAILGFALSEAMGLFCLMVAFLILFAM-------     143
Lvannamei VFGSLIIGYARNPSLKQQLFSYAILGFALSEAMGLFCLMMAFLLLFAF-------     114
Mjaponic  VFGSLIIGYARNPSLKQQLFSYAILGFALSEAMGLFCLMMAFLLLFAF-------     114
Msexta    TFGSLIIGYARNPSLKQQLFSYAILGFALSEAMGLFCLMMAFLLLFAF-------     130
Klactis   VFAALINGVSRNPSLKDTLFPFAILGFALSEATGLFCLMISFLLLYAV-------      76
Ecoli1c17 LGGKFLEGAARQPDLIPLLRTQFFIVMGLVDAIPMIAVGLGLYVMFAVA------      79
```

**Fig. 1** Shrimp *ATP9* subunit sequence. **A**) cDNA and deduced amino acid sequences. Untranslated sequences at 5′- and 3′-ends are *underlined*; *framed nucleotides* indicate start and end codons; *double underlined sequences* indicate mRNA stability sites, and *framed amino acids* show the signal peptide sequence. **B**) *ATP9* protein alignment includes *E. coli* 1C17 chain A sequence. *Black framed residues* indicate the signal peptide of the mature protein. Completely conserved residues are marked with a *black square*, highly conserved with an *asterisk*, and weakly conserved residues are marked with a *black dot*. *Bold marked letter* (D61 *E. coli*) is a suggested catalytic residue. R41, Q42/N42, P43, *underlined by a dotted line* indicate those residues located in the interhelical loop facing F1. *Double underlined and underlined residues* at both sites of the interhelical loop indicate transmembrane helices TMH1, and TMH2

A 680 bp sequence included 675 bp including the stop codon, and five additional bp between the stop codon and the polyA tail. The coding region includes an ATG start codon and a TAA stop codon according to the invertebrate mitochondrial codon code (Fig. 2A).

*L. vannamei atp6* cDNA sequence has 83 and 80% identity to the *atp6* genes from the mitochondrial genomes of *Penaeus notialis* and *P. monodon* (AF217843; X84350), and 97% to a partial mRNA *atp6* sequence from *L. vannamei* (DQ398573). This transcript as others coded in the mitochondria did not include untranslated sequences. Contrary to the shrimp *atp9* cDNA, the *atp6* transcript has a clear polyadenylation signal AATAAA. No ATTTA-rich regions were found, probably because different mechanisms acts in stabilizing and regulating the expression of mitochondrial coded transcripts. We found no differences between our cDNA sequence and the complete *atp6* gene, which was deposited in the GenBank as part of the complete mitochondrial genome of *L. vannamei* (NC_009626). Both sequences are 100% identical in the

**a**

```
ATGATAACAAATTTATTCTCAGTCTTTGATCCTACATCAAGAGTTCTTATACTCCCTCTTAACTGAATATCTACCTTCCTTGGAATGATATTTTTGCCTA 100
 M  M  T  N  L  F  S  V  F  D  P  T  S  S  V  L  M  L  P  L  N  W  M  S  T  F  L  G  M  M  F  L  P

TACTTTATTGAGCAATACCATCACGATGATCCCTATTATGAACTTTGATTACAAGAACTCTTCACAAAGAATTTAAAACTTTATTAGGTTCATCTCATTT 200
M  L  Y  W  A  M  P  S  R  W  S  L  L  W  T  L  I  T  S  T  L  H  K  E  F  K  T  L  L  G  S  S  H  F

TGGAACTACACTCATATTTGTTAGTCTTTTTAGCCTTATTGTTTTTAATAACTTTTTAGGTCTACTTCCATACGTTTTTACAAGCACAAGACATCTTACT 300
  G  T  T  L  M  F  V  S  L  F  S  L  I  V  F  N  N  F  L  G  L  L  P  Y  V  F  T  S  T  S  H  L  T

ATAACACTAGCTCTTGCCCTACCTTTATGAGTAGCCTTTATAATATTCGGATGAATTAACCACACTCAACATATGTTTGCTCATCTTGTTCCGCAAGGGA 400
 M  T  L  A  L  A  L  P  L  W  V  A  F  M  M  F  C  W  I  N  H  T  O  H  M  F  A  H  L  V  P  O  C

CTCCCGGAGCTCTTATACCTTTTATAGTATTAATTGAAACCATCAGAAATGTAATCCGACCTGGTACCTTAGCAGTGCGATTAGCAGCTAATATAATTGC 500
T  P  G  A  L  M  P  F  M  V  L  I  E  T  I  S  N  V  I  R  P  G  T  L  A  V  R  L  A  A  N  M  I  A

AGGCCACCTATTACTTACTCTTTTAGGAAGAACTGGTCCTTCCTTATCAGCTACATTGATTTCTATGCTTATTATTGGACAGATCCTATTATTAATTCTT 600
  G  H  L  L  L  T  L  L  G  S  T  G  P  S  L  S  A  T  L  I  S  M  L  I  I  G  O  I  L  L  L  I  L

GAAGCTGCTGTAGCAGTTATTCAGTCATATGTATTTGCAGTATTAAGAACCCTTTATGCTAGCGAAGTCACATAATAAACAAAAAAAA              680
 E  A  A  V  A  V  I  O  S  Y  V  F  A  V  L  S  T  L  Y  A  S  E  V  T
```

**b**

```
Fnotialis     MMTNLFSVFDPTSSIFMLPLNWVSTFLGVMFLPMLYWAMPSRWSLLWNLVTATLHKEFKTLLGSS-HFGTTLMFVSLFSLIVFNNFLGLLPYIFTSTSHL   99
Lvannamei     MMTNLFSVFDPTSSVLMLPLNWMSTFLGMMFLPMLYWAMPSRWSLLWTLITSTLHKEFKTLLGSS-HFGTTLMFVSLFSLIVFNNFLGLLPVIFTSTSHL   99
Mjaponicus    MMTNLFSVFDPTSSVLMLPLNWLSTFLGILFLPMLYWAMPSRWSLLWTMVSTTLHKEFKTLLGTS-HLGTTLMFVSLFSLIVFNNFLGLLPVIFTSSSHL   99
Pmonodon      MMTNLFSVFDPTSSLMNIPLNWLSTFLGVMFLPMMYWIMPSRWSLLWNLITSTLHKEFKILLGSS-HTGSTLMFVSLFTFIVFNNFLGLLPVIFTSTSHL   99
Plongicarpus MMTNLF SVFEPSSSLMNLPLNWMSTFIGLMFIPYLFWISPSRWSLLWTKINMALHKEFSTILGPS-QKSSTIIFVSLFSLIVFNNSLGLFPYIPTSSSHL  99
Dsimulans     MMTNLFSVFDPS-AIFNLSLNWLSTFLGILMIPSIYWLMPSRYNIVWNSILLTLHKEFKTLLGPSGHNGSTFIFISLFSLILFNNFMGLFPYIFTSTSHL   99
Dmelanogast   MMTNLFSVFDPS-AIFNFSLNWLSTFLGLLMIPSIYWLMPSRYNIMWNSILLTLHKEFKTLLGPSGHNGSTFIFISLFSLILFNNFMGLFPYIFTSTSHL   99
Aaegypti      MMTNLFSVFDPSTTILNLSLNWLSTFLGLLIIPSTYWLMPNRFQIIWNNILLTLHKEFKTLLGPNGHNGSTLMFVSLFSLIMFNNFMGLFPYIFTSTSHL   100
EcolilC17     ----------------------HGKSKLIAPLALTIFVWVFLMNL--------------------------MDLLPIDLLPYIAEH-VLGLPALRVVPSADV   53

Fnotialis     VMTLSLALPLWVAFMLFGWINHTQHMFAHLVPQG--TPGALMPFMVLIETISNVIRPGTLAVRLAANMIAGHLLLTLLGSTGP-SLSATLISMLIIGQIL   196
Lvannamei     TMTLALALPLWVAFMMFGWINHTQHMFAHLVPQG--TPGALMPFMVLIETISNVIRPGTLAVRLAANMIAGHLLLTLLGSTGP-SLSATLISMLIIGQIL   196
Mjaponicus    TMTLALALPLWLAFMIFGWVNHTQHMFAHLVPQG--TPGPLMPFMVLIETISNIIRPGTLAVRLAANMIAGHLLLTLLGSTGP-SLSMTLVSILIIGQIL   196
Pmonodon      IMTLALALPLWLAFMMFGWINHTQHMFAHLVPQG--TPDALMPFMVLIETISNVIRPGTLAVRLAANMIAGHLLLTLLGNTGP-SLSTTLVFLLIMTQIL   196
Plongicarpus AMTLTLSLPLWLTFMIYGWVNHTQHMFAHLVPQG--TPAVLMPFMVLIETISNVIRPGTLAVRLAANMMAGHLLLTLSGNTGP-SLNYYLLSILIFSQIL   196
Dsimulans     TLTLSLALPLWLCFMMYGWINHTQHMFAHLVPQG--TPAVLMPFMVCIETISNIIRPGTLAVRLTANMIAGHLLLTLLGNTGP-SMSYLLITFLLTAQIA   196
Dmelanogast   TLTLSLALPLWLCFMLYGWINHTQHMFAHLVPQG--TPAILMPFMVCIETISNIIRPGTLAVRLTANMIAGHLLLTLLGNTGP-SMSYILVTFLLMAQIA   196
Aaegypti      TLTLTLAFPLWLSFMLYGWICHTQHMFAHLVPQG--TPPVLMPFMVCIETISNVIRPGTLAVRLTANMIAGHLLMTLLGNTGPMSTSYIILSLILITQIA   198
EcolilC17     NVTLSMALGVFILILFYSIKMKGIGGFTKELTLQPFNHWAFIPVNLILEGVSLLSKPVSLGLRLFGNMYAGELIFILIAGLLPWWSQWILNVPWAIFHIL   153

Fnotialis     LLILEAAVAVIQSYVFAVLSTLYASEVT      224
Lvannamei     LLILEAAVAVIQSYVFAVLSTLYASEVT      224
Mjaponicus    LLILEAAVAVIQSYVFAVLSTLYASEVT      224
Pmonodon      LLILEAAVAVIQSYVFAVLSTLYASEVV      224
Plongicarpus LLLLESAVAVIQSYVFAVLSTLFASEIN      224
Dsimulans     LLVLESAVAMIQSYVFAVLSTLYSSEVN      224
Dmelanogast   LLVLESAVAMIQSYVFAVLSTLYSSEVN      224
Aaegypti      LLVLESAVAIIQSYVFAVLSTLYSSEVN      226
EcolilC17     IITLQAFIFMVLTIVYLSMASEER----      177
```

**Fig. 2** Shrimp *ATP6* subunit sequence. **A**) cDNA and deduced amino acid sequences. *Framed codons* indicate start and end codons; *double underlined sequence* of 5 bp indicate the untranslated region at 3′-end. **B**) *ATP6* protein alignment with crustacean, insect, and bacterial species. *E. coli 1C17* chain K was included. *Black framed residues* R160 indicate the suggested site which interacts with *ATP9* subunit. Completely conserved residues are marked in *bold characters*

coding region, however 1 bp difference was observed in the 3′-untranslated region of 5 bp found in the cDNA sequence between the stop codon and the poly A tail, which can be TAACC or TAAAC in different individuals. The coding sequence corresponds to a protein of 224 amino acid residues, with a predicted molecular mass of 24.7 kDa and an isoelectric point of 7.62. A S residue at position 7, which is highly conserved in crustacean species, is proposed to be a possible proteolytic processing site (Guelin et al. 1991). Also, at positions 145, 149, 200, and 211 of the *ATP6* protein, we found conserved residues in the shrimp sequence that have been suggested to be implicated in oligomycin resistance in yeast and fungi species as *Saccharomyces cerevisiae*, and *Candida parapsilopsis* (Fig. 2B).

## *ATP9-ATP6* protein model analysis

The theoretical tridimensional model based on the alignment of the sequences and 3-D modeling contains three *ATP9* and one *ATP6* subunits, one of the *ATP9* subunits interacting with *ATP6* (Fig. 3). The alignment of the mature *ATP9,* after removal of the signal peptide, showed that the

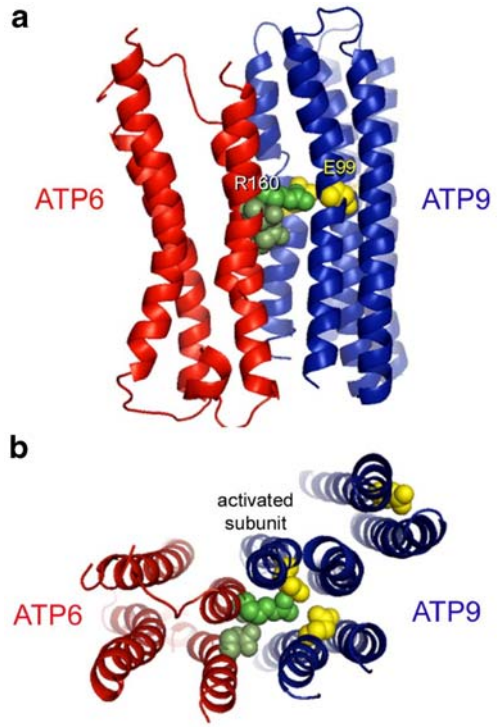


**Fig. 3** Molecular model of *ATP9-ATP6* subcomplex from shrimp *L. vannamei*. **a** Ribbon lateral view, and **b** ribbon front view of subunit *ATP6* complexed with three *ATP9* subunits. The predicted functional residues are *marked* in both subunits, R160 from *ATP6*, and E99 from *ATP9*

polypeptides are all approximately of the same size. We propose that the monomeric subunit *ATP9* of shrimp, folds in a hairpin-like structure of two extended transmembrane α-helices (TMHs), that include the conserved residues R79-N80-P81 that are also found in the interhelical loop of the hairpin in vertebrates and some insects species (Hong and Pedersen 2003; Figs. 1 and 3).

We identified in the ATP9 protein of *L. vannamei*, that E99 is the main functional residue, which is located in the TMH2 and is suggested to be the primary proton carrier that binds protons and release them at the center of the membrane, as commonly observed in yeast and vertebrates. In bacteria, this residue is commonly a D, and the difference in side chain size of E and D allowed us to predict differences in the ATP9 stoichiometry in crustacea.

The number of *ATP9* molecules in the ring is still debated even in the most studied species as *E. coli*, whose *ATPc* ring structure has been reported to include ten molecules (Fillingame et al. 2002). It is also known that the ATP-synthase Fo complex is comprised of 9–12 *ATP9* subunits (Andersson et al. 1997; Rubinstein et al. 2003). Thus we propose that the larger side chain of *ATP9*-E99 residue from the shrimp structure at the interface with *ATP6* suggests that a small number of subunits are packed in to the oligomeric ring of ATP9.

The *ATP6* protein from the predicted model of shrimp is a highly hydrophobic protein, with a molecular mass of 24.7 kDa, similar to that of bovine *ATP6* (24.8 kDa; Walker et al. 1991), but smaller than that of *E. coli* (Long et al. 1998). As observed in bacterial and vertebrates enzymes (Fillingame et al. 2002; Rubinstein et al. 2003), we suggest there is a single *ATP6* subunit in the enzyme complex of shrimp. According to Vick and Ishmukhametov (2005) observations, the key functional residue of subunit *a* in bacteria (*ATP6* in eukaryotic organisms), is R210, which functions through its interactions with the subunits *c* oligomer in the proton channel. The alignment of crustacean and bacteria (*E. coli*, AAA24731.1) amino acidic sequences, showed R160 to be positioned at this site suggesting that this highly conserved residue between invertebrate species, could be the one in crustacean species *ATP6* that interacts with the ring of *ATP9* subunits (Fig. 1B).

The key feature of the R residue in bacteria is thought to be the positive charge (Ishmukhametov et al. 2008), thus shrimp R160 will accomplish this characteristic suggesting that positive charges are needed for attraction between subunits leading to rotation. Some other conserved amino acid residues were observed in shrimp subunit *ATP6* such as E146 (*E.coli*: E196), L161 (*E.coli*: L211), N164 (*E.coli*: N214), and residue Q208 (*E.coli*: L259) all together are reported in the PROSITE pattern ([GSTA]-R-[NQ]-P-x(5)-{A}-x-{F}-x(2)-[LIVMFYW](2)-x(3)-[LIVMFYW]-x-[DE],PS00605). The pair of residues E219 and H245 (*E. coli* sequence) have been proposed to control a proton access channel (Vick and Ishmukhametov 2005). These two residues are near-neighbors in the structure 1C17, and a double mutant E219H/H245E exhibits marginal activity. The shrimp model has inverted positions of H, with a polar residue Q or E, i.e. shrimp H169 in the position of *E.coli*: E219, and shrimp Q194 in the position of *E.coli*:H245. Such structural residue swapping suggests an evolutionary conservation of subunit interactions.

## *Atp9* and *atp6* mRNA levels in shrimp tissues

The steady state mRNA levels were evaluated in five different tissues from three organisms with triplicates. Standard curves were constructed for *atp9*, *atp6* and *L8* showing similar efficiencies of 100.0, 101.7, and 103.0%, respectively. Each of the melting curves generated at the end of the PCR reaction contained a single PCR product for each gene in all samples. Figs. 4a and b show *atp9* and *atp6* mRNA levels as the expression ratio (ER), relative to the *L8* ribosomal protein transcripts. *Atp9* differences of 80 and 77% between gills and muscle compared to the *atp9* mRNA levels of midgut gland were found. Also, the *atp6* mRNA levels varied 78% between the maximum and minimum values observed in muscle and midgut gland, respectively. Both

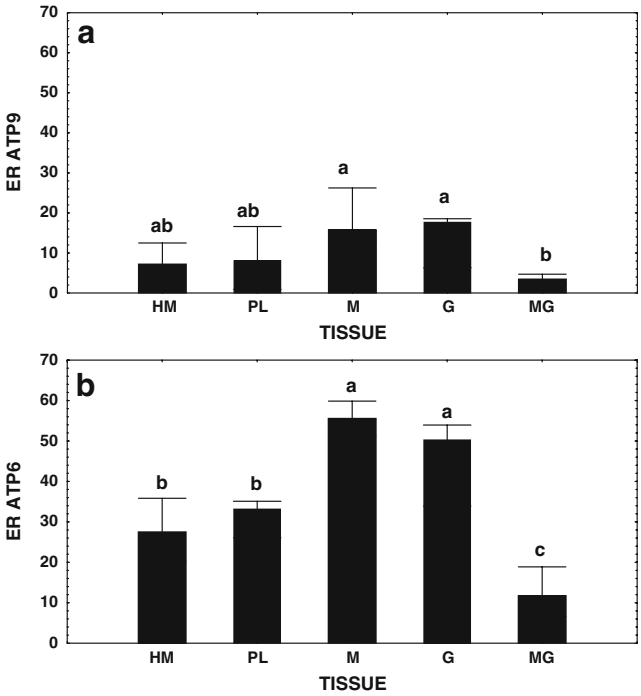


**Fig. 4** Relative expression ratio (*ER*). **a**) *Atp9*, and **b**) *atp6* transcripts relative to ribosomal protein *L8* in five different shrimp tissues from seven hundred nanograms of total RNA from (*HM*) haemocytes, (*PL*) pleopods, (*M*) muscle, (*G*) gills, and (*MG*) midgut gland. Data represent median values ±25–75% min and max values

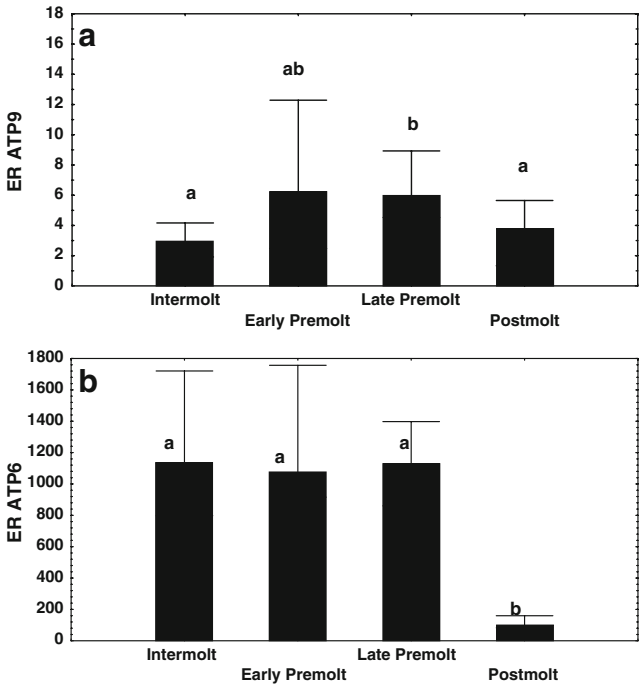


**Fig. 5** Relative expression ratio (*ER*). **a**) *Atp9*, and **b**) *atp6* transcripts relative to *L8* in the midgut gland of shrimp at different molt stages. Data represent median values ±25–75% min and max values

subunits were transcribed in tissues following a similar sequence: muscle = gills > pleopods > hemocytes > midgut gland (Fig. 4), suggesting the existence of a coordinated abundance pattern for both *atp9* and *atp6* subunits in the analyzed tissues.

## *Atp9* and *atp6* mRNA levels at different molt stages

Expression levels of *atp9* and *atp6* in the midgut gland of five shrimp at four different molt stages were evaluated by triplicate. Standard curves were constructed with efficiencies of 100.3% (*atp9*), 99.6% (*atp6*), and 101.0% (*L8*). Melting curves also generated specific products for each gene. Results, expressed as a relative expression ratio (ER) are shown in Fig. 5a and b.

Crustaceans molt cycle implies exuviation of the old exoskeleton and a subsequent synthesis of a new cuticle. The complete process requires the use of considerable energy, and therefore, the need to synthesize and use ATP (Dall et al. 1990). During intermolt and premolt stages (specifically early premolt, stages $D_1$ to $D_3$; Madhyastha and Rangneker 1974), glycogen granules derived from food and from resorption of the old cuticle accumulate in the midgut gland of shrimp. At these stages, shrimp are actively feeding to increase reserves in the midgut gland to endure when feeding ceases and a new cuticle is synthesized (ecdysis and postmolt; Dall et al. 1990). At intermolt, early premolt, and late premolt stages we detected higher values and statistical differences in mRNA levels compared to postmolt stage only in *atp6*, but not in *atp9* (Figs. 5a and b). This observation suggests that molecules of the ATP synthase complex from shrimp are positively or negatively controlled in the mitochondrial apparatus of the midgut gland cells, responding to different physiological stimuli as means of modulating the relative content of ATP-synthase complexes, to synthesize/ hydrolyze ATP to meet the energy demand as observed in rats (Andersson et al. 1997).

Significant decrease of *atp6* and *atp9* mRNAs levels were observed between late-premolt and postmolt stages, after shrimp had lost the old exoskeleton and had not been able to handle food during 2 or 3 days (Figs. 5a and b). This agrees with the decreasing mRNA levels and enzyme activity of proteases such as trypsins in the midgut gland of shrimp at the post molt stage (Muhlia-Almazan and Garcia-Carreño, 2002; Sanchez-Paz et al. 2003). After molting there is no food to be digested in the midgut gland, shrimp are buried and not actively swimming, energy has to be saved to accomplish the synthesis of the new cuticle, and we suggest the biogenesis of the ATP-synthase complexes may be down-regulated as a response to the general metabolic state of shrimp.

Contrary to the results from different tissues, no clear coordinated expression patterns were found between *atp9* and *atp6* mRNA levels in shrimp at different molt stages

(Fig. 5). In addition we found that mitochondrial transcripts *atp6* were higher than nuclear *atp9* in all the shrimp tissues and molt stages. These observations could be partially explained by the larger and varying number of mitochondria in the different tissues, as previously suggested (Robin and Wong 1988, see discussion). However, to deeply understand these results, we compared both genes from nuclear and mitochondrial origin as markers for mitochondrial biogenesis, and we calculated a ratio of mitochondrial/nuclear mRNA levels at each evaluated tissue and molt stage (Table 2).

We detected larger differences in the *atp6*/*atp9* ratios at different molt stages, than those between different tissues (Table 2). We suggest that tissues from the same shrimp, under a common physiological condition, will have low differences between *atp6*/*atp9* ratios. However, in different individual organisms at quite different energetic and physiological conditions, as observed between molt stages, the differences in *atp6*/*atp9* ratios will be larger even in the same tissue as observed. Thus, the "coordinated or non-coordinated" changes observed between mRNA levels of ATP-synthase subunits will be the result of more than one regulatory mechanism acting at different levels in response to environmental changes and also in response to endogenous physiological conditions.

## Discussion

Although it seems that the ATP-synthase complex from distant species in a phylum have highly conserved elements and molecular characteristics, species from different environments and metabolic needs have proved to display special and uncommon characteristics in their ATP-synthase complex structure and function (van Lis et al. 2003; Morales-Sainz et al. 2008). The scarce information about crustaceans' ATP-synthase does not allow comparisons among closely related species, thus our predictions about this enzyme structure and their implications in shrimp are the basis to further and deeper studies to confirm the discussed elements of this research.

**Table 2** Ratio of mitochondrial/nuclear mRNA levels at each evaluated tissue and molt stages

| | *atp6*/*atp9* ratio |
|---|---|
| Tissue | |
| Hemocytes | 3.8 |
| Pleopods | 4.16 |
| Muscle | 3.5 |
| Gills | 2.84 |
| Midgut gland | 3.35 |
| Molt stage | |
| Intermolt | 386 |
| Early premolt | 173 |
| Late premolt | 186 |
| Post molt | 27 |

We investigated two hydrophobic membrane proteins from shrimp that are suggested to be involved in protons translocation in the Fo sector of the multimeric complex ATP-synthase: *ATP6* and *ATP9*. Studies of the structure of these proteins in bacteria have revealed four important amino acid residues involved in proton translocation and interaction between both subunits: *ATPc*-D61,and *ATPa*-R210, E219, and H245 (Cain and Simoni 1989; Long et al. 1998; Vick and Ishmukhametov 2005). These residues are *ATP9*-E99, and *ATP6*-R160, H-169, Q-194 in the shrimp *L. vannamei*. We believe that these conserved elements in the protein model may allow the enzyme to function in a similar way as it has been proposed in the most studied models as bacteria. According to the *E. coli* protein model proposed by Fillingame et al. (2000; 2002), during the rotary catalytic mechanism in which protons transport is coupled to rotation of the *ATPc* ring in the Fo sector, the conformation of *ATPa-c* helical interactions change. In the crustacean predicted model, we observed the TMH1s from the three subunits in the *ATP9*-ring to be on the inside part of the ring, and the TMH2s on the outside part of the ring (Fig. 3b). The TMH2s, where E99 residues are placed must swivel, allowing the interaction with the R160 residue of shrimp *ATP6* subunit agreeing with the *E. coli* model.

According to Gay and Walker (1985), the expression of *atp9* genes was shown to be tissue-specific in the bovine. This also agrees with the results of Andersson et al. (1997) and Himeda et al. (2000) who evaluated mRNA levels of this subunit and other nuclear ATP-synthase subunits in different rat tissues. In 8-week-old rats, Himeda et al. (2000) found that the mRNA concentration of *atp9* was lower in the liver compared to the brain, heart and kidney, assuming differences are related to tissue function. In 1995, Houstek et al. (1995) found that in rat tissues, the content of ATPase complexes in the mitochondrial membranes correlates with changes observed in the *atp9* mRNAs. Later, Andersson et al. (1997) suggested that the expression of *atp9* genes, but not that of the all other subunits of ATP-synthase, appears to regulate the level of the entire ATPase complex.

Thus, assuming this correlation exists, we may propose that levels of *atp9* and *atp6* mRNAs are related to each tissue function; and that muscle and gills cells, have higher contents of ATP-synthase complexes that can be related with the energy required by each tissue to accomplish its functions. Thus, muscle and gills, that are active in locomotion and respiration, have high energy requirements for shrimp to deal with ocean currents, flotation, or looking for food and breathing.

As we observed, mitochondrial *atp6* transcripts were also higher in all molt stages than nuclear ones (*atp9*), therefore, the differences could be related to the larger and different number of mitochondria per cell found in different tissues, compared to a single copy of the nuclear genes. Robin and Wong (1988), suggested that the number of mitochondrial DNA molecules (mtDNA) per mitochondria is essentially constant in all cell types (2.6±0.30 for mammalian cells), however, the number of mitochondria per cell widely differ from tissue to tissue.

According to the mitochondrial DNA structure, and to the number of promoter regions in the mtDNA from each species, genes are commonly transcribed stoichiometrically as large polycistronic mRNAs (Duborjal et al. 2002). However, (Heddi et al. 1999) suggested that under specific inhibitory, stress or pathological conditions, the levels of only a few of the mitochondrial transcripts may change. In agreement to these suggestions we detected larger differences among tissues and molt stages of *atp6* transcripts than for *atp9*. These differences can be due to the different origin of the genes, and additionally because *atp6* has been shown to be one of the most regulated subunits from the ATP-synthase complex under stress conditions (Dubot et al. 2004); while *atp9* has been reported as part of the "low transcript genes" group from the ATP-synthase of rats (Sangawa et al. 1997).

Studying multimeric enzymes has inherent difficulties due to their elaborate structure and the complex mechanisms involved in their synthesis, assembling and functioning. Moreover, mitochondrial ATP-synthases require for their biosynthesis a series of coordinated events between mitochondria and nucleus. Future research must be directed to deeply analyze those regulatory elements in shrimp genomes.

To our knowledge the total amount of *atp6* and *atp9* mRNAs from the ATP-synthase complex in any tissue or physiological condition is strongly related to the energy requirement of shrimp, and to the number of ATP-synthase molecules per mitochondria per cell at any specific time. Furthermore, ATP synthesis/hydrolysis is the consequence of various regulatory mechanisms acting at different levels. Thus, although transcriptional regulation is assumed to be one of the major mechanisms regulating protein synthesis in eukaryotes, it seems to be neither unique nor most important in the shrimp OXPHOS systems. Highly specialized mechanisms are suggested to operate in species more deeply studied, such as vertebrates and bacteria. The information obtained in this work provides basic elements for future studies that may be addressed to evaluate biochemical properties of shrimp $F_0F_1$ ATP-synthase under the particular physiological processes that marine crustaceans face during their life cycle. Additionally, efforts must be made to resolve the precise locations and roles of other supernumerary subunits present in mitochondrial ATP-synthase complexes of crustaceans and to understand the mechanisms controlling transcriptional and translational processes during the biogenesis of crustacean ATP-synthases.

**Acknowledgements** AMA acknowledges support from International Foundation for Science (IFS, grant A/3867-1), and Consejo Nacional de Ciencia y Tecnologia (CONACYT, National Council for Research and Technology, Mexico) for grant 48989-Z. OMC thanks CONACYT for a graduate scholarship. We also thank Drs. Arturo Sanchez-Paz, Diego Gonzalez-Halphen and Maria A. Islas-Osuna for critical reading of the manuscript.

## References

Altschull SF, Gish W, Miller W, Meyers EW, Lipman DJ (1990) J Mol Biol 215:403–410
Andersson U, Houstek J, Cannon B (1997) Biochem J 323:379–385
Bacca H, Huvet A, Fabioux C, Daniel JY, Delaporte M, Pouvreau S, van Wormhoudt A, Moal J (2005) Comp Biochem Physiol 140B:635–646
Boyer PD (1997) Ann Rev Biochem 66:717–749
Brown-Peterson NJ, Manning CS, Patel V, Denslow ND, Brower M (2008) Biol Bull 214:6–16
Caggese C, Ragone G, Perrini B, Moschetti R, De Pinto V, Caizzi R, Barsanti P (1999) Mol Gen Genet 261:64–70
Cain BD, Simoni RD (1989) J Biol Chem 264:3292–3300
Chan SM, Rankin SM, Keeley LL (1988) Biol Bull 175:185–192
Claros MG, Vincens P (1996) Eur J Biochem 241:779–786
Clavero-Salas A, Sotelo-Mundo RR, Gollas-Galván T, Hernández-López J, Peregrino-Uriarte AB, Muhlia-Almazán A, Yepiz-Plascencia G (2007) Fish Shellfish Immunol 23:459–472
Dall W, Hill BJ, Rothlisberg PC, Sharples DJ (1990) The Biology of Penaeidae. Academic, USA
DeWoody JA, Chesser RK, Baker RJ (1999) J Mol Evol 48:380–382
Duborjal H, Beugnot R, Mousson de Camaret B, Issartel JP (2002) Gen Res 12:1901–1909
Dubot A, Godinot C, Dumur V, Sablonniere B, Stojkovic T, Cuisset JM, Vojtiskova A, Pecina P, Jesina P, Houstek J (2004) Biochem Biophys Res Comm 313:687–693
Dyer MR, Walker JE (1993) Biochem J 293:51–64
Fillingame RH, Jiang W, Dmitriev OY (2000) J Bioenerg Biomembr 32(5):433–439
Fillingame RH, Angevine CM, Dmitriev OY (2002) Biochim Biophys Acta 1555:29–39
Garcia-Machado E, Dennebouy N, Suarez MO, Mounolou JC, Monnerot M (1996) CR Acad Sci Paris-Sci la Vie/Life Sci 319:473–486
Gay NJ, Walker JE (1985) EMBO J 4:3519–3524
Godbout R, Bisgrove DA, Honore LH, Day RS (1993) Gene 123:195–201
Guelin E, Guerin M, Velours J (1991) Eur J Biochem 197:105–111
Heddi A, Stepien G, Benke PJ, Wallace DC (1999) J Biol Chem 274:22968–22976
Higuti T, Kuroiwa K, Kawamura Y, Morimoto K, Tsujita H (1993) Biochim Biophys Acta 1172:311–314
Himeda T, Morokami K, Arakaki N, Shibata H, Higuti T (2000) Eur J Biochem 267:6938–6942
Hong S, Pedersen PL (2003) J Bioenerg Biomembr 35:95–120
Houstek J, Andersson U, Tvrdik P, Nedergaard J, Cannon B (1995) J Biol Chem 270(13):7689–7694
Ishmukhametov RR, Pond JB, Al-Huqail A, Galkin MA, Vik SB (2008) Biochim Biophys Acta 1777:32–38

Itoi S, Kinoshita S, Kikuchi K, Watabe S (2003) Am J Physiol 284: R153–R163
Jones TA, Zou JY, Cowan SW, Kjeldgaard M (1991) Acta Crystallogr A 47:110–119
Long JC, Wang S, Vik SB (1998) J Biol Chem. 273(26):16235–16240
Madhyastha MN, Rangneker PV (1974) Broter Serie Trimestral: Cienc Nat 43:135–149
Malter JS, Hong Y (1991) J Biol Chem 266:3167–3171
Morales-Sainz L, Escobar-Ramirez A, Cruz-Torres V, Reyes-Prieto A, Vazquez-Acevedo M, Lara-Martinez R, Jimenez-Garcia LF, Gonzalez-Halphen D (2008) Biochim Biophys Acta 1777:202–210
Muhlia-Almazan A, Garcia-Carreño FL (2002) Comp Biochem Physiol 133B:383–394
Nagley P (1988) TRENDS Genetics 4:46–52
Rastogi VK, Girvin ME (1999) Nature 402:263–268
Robin ED, Wong R (1988) J Cell Physiol 136:507–513
Rubinstein JL, Walker JE, Henderson R (2003) EMBO J 22:6182–6192
Sambrook J, Russell DW (2001) Molecular Cloning: A Laboratory Manual. Cold. Spring Harbor Laboratory, USA
Sanchez-Paz A, García-Carreño F, Muhlia-Almazán A, Hernández-Saavedra NY, Yepiz-Plascencia G (2003) J Exp Mar Biol Ecol 292:1–17
Sangawa H, Himeda T, Shibata H, Higuti T (1997) J Biol Chem 272:6034–6037
Sardiello M, Tripoli G, Romito A, Minervini C, Viggiano L, Caggese C, Pesole G (2005) TRENDS Genetics 21:12–16
Shen X, Ren J, Cui Z, Sha Z, Wang B, Xiang J, Liu B (2007) Gene 403(1–2):98–109
van Lis R, Atteia A, Mendoza-Hernandez G, Gonzalez-Halphen G (2003) Plant Physiol 132:318–330
Vargas-Albores F, Guzmán-Murillo MA, Ochoa J-L (1993) Comp Biochem Physiol 106A:299–303
Vick SB, Ishmukhametov RR (2005) J Bioener Biomembr 37:445–449
Viebrock A, Perz A, Sebald W (1982) EMBO J 1(5):565–571
Walker JE, Lutter R, Dupuis A, Runswick MJ (1991) Biochemis 30:5369–5378
Wang H, Oster G (1998) Nature 396:279–282
Wang B, Li F, Dong B, Zhang C, Xiang J (2006) Mar Biotechnol 8 (5):491–500
Wilson K, Cahill V, Ballment E, Benzie JAH (2000) Mol Biol Evol 17:863–874
Yotov WV, St-Arnaud R (1993) Biochem Biophys Res Commun 191:142–148